Si-H clusters, defects, and hydrogenated silicon

R. O. Jones
Institut für Festkörperforschung, Forschungszentrum Jülich, D-52425 Jülich, Germany

B. W. Clare and P. J. Jennings
School of Mathematical and Physical Sciences, Murdoch University, Murdoch, WA 6150, Australia
(Received 2 April 2001; published 6 September 2001)

All-electron density functional methods have been used to calculate the structures and energies of silicon/hydrogen clusters with up to 148 atoms. Vibration frequencies are calculated for those clusters with less than 75 atoms. In addition to hydrogen-terminated clusters based on the structures of bulk Si, we study structures involving vacancies, divacancies, and additional H atoms. The results are compared with earlier work and provide vibration fingerprints that should aid the interpretation of measurements (such as infrared spectra) of hydrogenated crystalline and amorphous silicon.

DOI: 10.1103/PhysRevB.64.125203 PACS number(s): 78.30.Ly, 61.72.Ji, 63.22.+m, 71.55.Cn

I. INTRODUCTION

The electrical and optical properties of semiconductors are determined to a large extent by structural defects. In the case of silicon, there have been countless studies of intrinsic defects (including the self-interstitial I and the vacancy V) as well as impurities, and recent references to work on the structure and dynamics of defects in crystalline Si are given in Ref. 1. It is only in recent years that detailed information about the structures and interactions of these defects has become available.

The essential features of the electronic structure of the Si vacancy are well established.[2] The removal of an atom from bulk Si results in four dangling bonds, with a nondegenerate A_1 level overlapping the valence band and a triply degenerate (T_2) level in the energy gap. One of the T_2 levels is doubly occupied in the neutral vacancy, and a Jahn-Teller distortion from $T_d \rightarrow D_{2d}$ symmetry results. Density functional calculations confirm the existence of Jahn-Teller distortions. However, the results show many differences in detail,[1,3–7] and both the atomic arrangement and the formation energy converge extremely slowly with the size of the supercell and the number of k points in the Brillouin zone.[5] Large Jahn-Teller distortions have also been found near divacancies in crystalline Si.[8,9]

The role of defects is crucial to the properties of amorphous and microcrystalline silicon (a-Si and μc-Si, respectively). These materials, which are of great interest for use in solar cells and optoelectronic devices such as color sensors, contain typically 10% hydrogen, which diffuses rapidly and interacts with defects, altering the structure, energy spectrum, and properties. The role of defects in a-Si produced by glow discharge is particularly important, since long exposure to light can lead to a substantial decrease in the photoconductivity. This effect, discovered by Staebler and Wronski,[10] limits the possible applications of this material. These changes can be reversed by annealing above 150 °C, where hydrogen diffusion becomes important, and defects associated with H atoms have often been invoked to explain the effect.[11] The formation and breaking of Si-Si and Si-H bonds are often assumed to be parts of the degradation mechanism,[11–14] and there have been many studies of the interaction of H atoms with defects in Si. In particular, the interaction of vacancies in Si with one to four H atoms ($VH_n, n=1,4$) has been studied by photoluminescence,[15] Fourier transform infrared (FTIR) spectroscopy,[16,17] and electron paramagnetic resonance (EPR).[16,18] Hydrogen phenomena in hydrogenated amorphous Si have been reviewed recently by Beyer.[19]

Density functional (DF) calculations have been used in many studies of defects in bulk semiconductors, including hydrogen-terminated clusters based on the bulk Si structure.[3] Structures generated in previous simulations of a-Si have been adopted (a) by Peressi *et al.*,[20] to study the formation and interchange of defects in amorphous and hydrogenated amorphous Si, and (b) by Silvestrelli *et al.*[21] in their study of defect configurations in a-Si. Cluster models have been used to simulate the local properties of extended systems, including those with defects.[22] It has been possible to calculate the electronic structure of passivated Si clusters with up to 800 atoms,[23] although the geometric structures were not optimized. Combined density functional/molecular dynamics calculations have been used recently to show pressure-induced amorphization in a $Si_{35}H_{36}$ cluster.[24]

In earlier work,[25] the Murdoch group estimated the energies required to break Si-H bonds in molecules related to the silanes SiH_4 and Si_2H_6 using Hartree-Fock calculations with and without estimates of the correlation energy obtained from second-order Møller-Plesset perturbation theory (MP2). These calculations suggested that both positive and negative charges reduce the strength of Si-H and Si-Si bonds. A semiempirical quantum chemical method (AM1)[26] was also used to calculate the vibration spectra and electronic densities of states for Si/H clusters, including defect structures with two and four additional H atoms. A comparison of the calculated vibration spectra with infrared absorption measurements on hydrogenated a-Si showed both similarities and discrepancies, but indicated that such models could be valuable in interpreting IR and other data.

These studies are extended here by performing all-electron DF calculations on clusters of Si and H [Si_mH_n, also denoted (m,n)] ranging in size from (10,16) to (84,64).

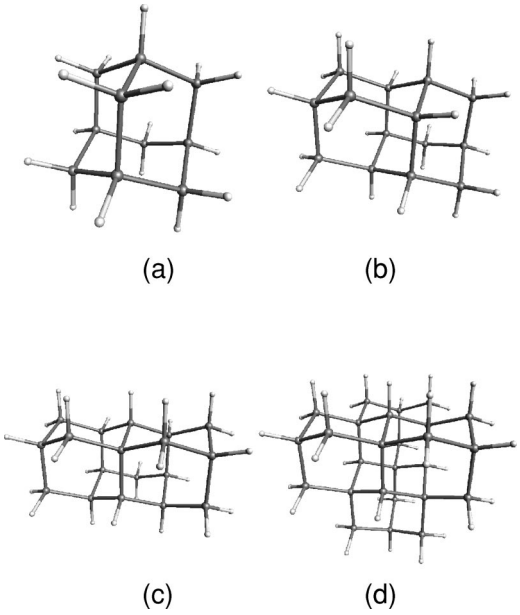

FIG. 1. Si/H clusters: (a) Si-adamantane $Si_{10}H_{16}$ (10,16); (b) Si-diamantane (14,20); (c) Si-triamantane (18,24); (d) Si-pentamantane (26,32).

The structures, which are derived from tetrahedrally coordinated fragments of crystalline Si with the dangling bonds passivated by H atoms, should resemble the structures found in hydrogenated μc-Si and may show local similarity to structures of hydrogenated a-Si. Hydrogen atoms are used both to saturate the bonds in atoms on the cluster surface and to form hydrogen aggregates near vacancies. We also calculate the energy required to transfer an H atom from a ''surface'' to an internal site, and the energies of two different structures with pairs of vacancies. The calculational method is free of adjustable parameters and has been used previously to calculate the structures, vibration frequencies, and energy differences in many smaller clusters.[27] In the context of Si-H clusters, the results can be used to assess the reliability of semiempirical methods, such as the AM1 method, which can be used to study the properties of much larger clusters than are presently accessible to DF methods.

Section II describes the methods used in these calculations, and the results are given in Sec. III. Our concluding remarks are presented in Sec. IV.

II. METHOD OF CALCULATION

The clusters shown in Figs. 1–3 may be viewed as fragments derived from the bulk Si structure, with all dangling bonds saturated with H atoms. The first four are Si analogs of the polymantane hydrocarbons $C_{4n+6}H_{4n+12}$, and we refer to them by the names adamantane [(10,16), 1(a)], diamantane [(14,20), 1(b)], triamantane [(18,24), 1(c)], and pentamantane [(26,32), 1(d)]. The two largest clusters are not in this series, but we use the names ''decamantane'' [(35,36), 2(a)] and ''superpolymantane'' [(84,64), 3(a)]. The number of the different bond types in these structures is shown in Table I, where we see that the number of H neighbors of the Si atoms changes nonmonotonically with increasing cluster size.

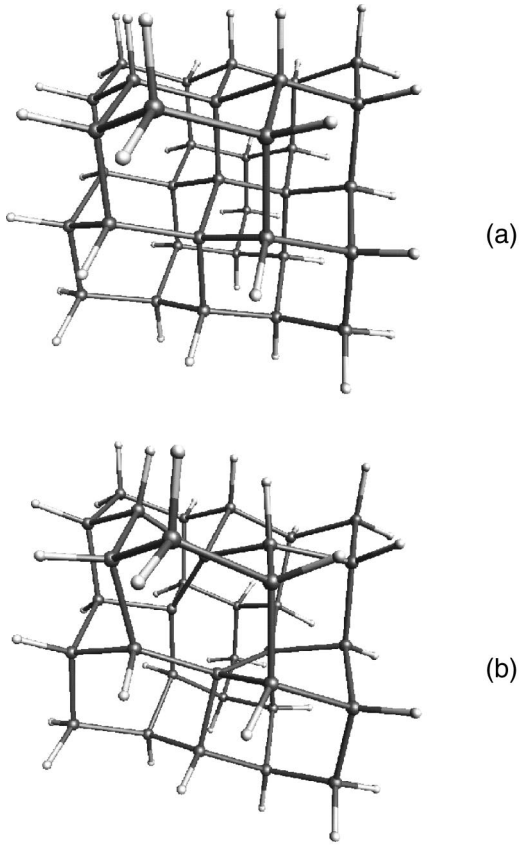

FIG. 2. Si/H clusters: (a) Si-decamantane (35,36); (b) ''vacancy'' (34,36).

In addition to clusters derived from the structure of bulk Si, we have considered several defect structures. These include those derived from decamantane by removing a single Si atom [(34,36), 2(b)], and by adding one, two, three, and four H atoms to this vacancy [Figs. 4(a)–4(d)]. Finally, we have considered two structures derived from superpolymantane by removing different pairs of Si atoms [3(b) and 3(c)].

Initial geometries were obtained using two calculation schemes: (a) the MOPAC quantum chemical package[28] and the AM1 Hamiltonian.[29] Several such structures have been described in Ref. 30, which also presented electronic densities of states and normal modes of vibration. (b) Combined molecular dynamics/density functional calculations[31] were used with a simulated annealing strategy to ensure that structures did not correspond to shallow local minima in the energy surface. The latter calculations use periodic boundary conditions, a nonlocal pseudopotential of the Trouiller-Martins form,[32] a plane wave basis with a kinetic energy cutoff of 35 a.u., and a single point ($\mathbf{k}=0$) in the Brillouin zone.

The geometries so found were used as input to DF calculations using all-electron basis sets of double-zeta (DZVP) and triple-zeta (TZVP) quality, and the local spin density (LSD) approximation for the exchange-correlation energy.[33] The structures were optimized without restrictions on symmetry (all atoms were allowed to relax) until the largest component of the gradient on any atom was less than 5×10^{-4} Hartree atomic units. In some cases these structures were

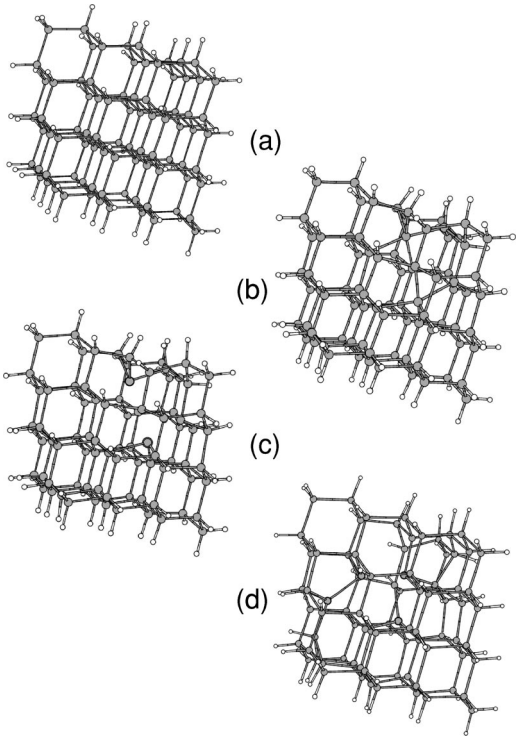

FIG. 3. Si/H clusters: (a) Si-superpolymantane (84,64); (b) (82,64) divacancy, all-electron calculations; (c) (82,64) divacancy, CPMD calculations; (d) (82,64) vacancy pair. In (c) the atoms with the darker circles are the nearest neighbors of the missing pair of atoms.

used as input to further simulated annealing calculations, which were followed again by all-electron optimization. The distributions of the energy eigenvalues were determined for the final structures. Vibration frequencies and the corresponding infrared intensities were determined from analytic expressions for the first and second derivatives with respect to the nuclear coordinates and external electric fields.[34] The six lowest frequencies—corresponding to rotations and translations—were projected out, and the eigenvectors corresponding to each frequency have been viewed graphically. Memory requirements of the program rule out vibration frequency calculations on the clusters related to superpolymantane (148 atoms), and the calculations of vibration frequencies of systems related to decamantane were possible with the DZVP basis alone.

The CPMD pseudopotential method and the all-electron calculations using DZVP and TZVP lead to a remarkably consistent picture of the structures and energy *differences* in all systems, apart from the neutral divacancy discussed in Sec. III B 1. Unless otherwise stated, the results given below are for all-electron calculations with the DZVP basis. All vibration frequencies are represented by a Gaussian peak with full width at half maximum (FWHM) of 10 cm^{-1}, a value also used in earlier work.[30] Energy eigenvalue densities of states are obtained by using a Gaussian broadening (FWHM) of 1 eV.

TABLE I. Atom neighbors in Si_mH_n clusters (m,n). The number of bonds of Si atoms with zero, one, and two H atoms is shown.

	(10,16)	(14,20)	(18,24)	(26,32)	(35,36)	(84,64)
Si-H_0 bonds	0	0	1	6	5	26
Si-H_1 bonds	4	8	10	8	24	52
Si-H_2 bonds	6	6	7	12	6	6

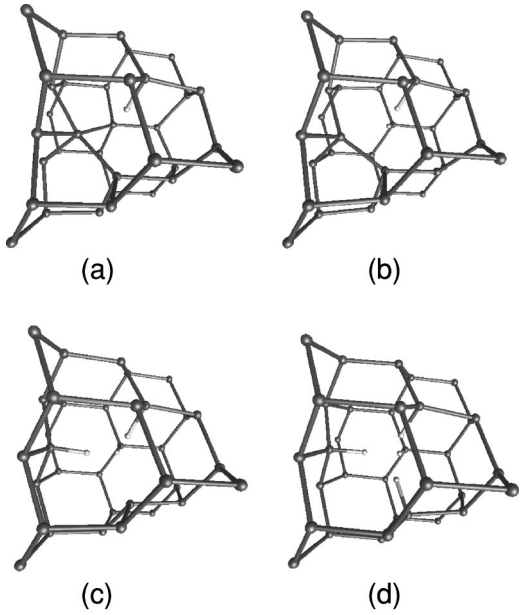

FIG. 4. Defect Si/H clusters without external H atoms: (a) (34,37); (b) (34,38); (c) (34,39); (d) (34,40).

III. RESULTS

In this section we present the results of our calculations. We discuss first the clusters without defects, i.e., the silicon analogs of the hydrocarbons adamantane (10,16) to superpolymantane (84,64), followed by the effects of removing Si atoms and/or adding H atoms. The coordinates of all structures may be obtained from the first author.

A. Clusters without defects

1. Structures

We consider in this section H-terminated clusters based on the diamond structures of Si. The optimized Si-Si bond lengths in all clusters lie in a narrow range 2.33 Å to 2.34 Å, in very good agreement with the bulk value (2.352 Å), and the Si-H bond lengths lie between 1.50 Å and 1.51 Å. All bond angles lie between 109° and 110°, very close to the bond angles in tetrahedral structures (109.47°).

In order to show the variation of bond lengths and angles in Si/H systems with different coordination, we show some results for the small molecules silylidene SiH, silylene SiH_2, silane SiH_4, Si_2H_4, and Si_2H_6 in Table II. These calculations used the DZVP basis and the LSD approximation to the exchange-correlation energy. Also shown are the frequencies and type of the vibration modes in these molecules and the

TABLE II. Structure (bond lengths in Å) and vibration frequencies (cm^{-1}) of Si/H molecules. LSD values are given, with BLYP values (Ref. 35) for SiH and SiH_2 in parentheses. The vibration frequencies in SiH_4, Si_2H_4, and Si_2H_6 are shown for strongly infrared active modes only. Experimental values for SiH, SiH_2, and SiH_4 [square brackets] are from the compilation of Ref. 36.

	SiH	SiH_2	SiH_4	Si_2H_4	Si_2H_6
$d_{\text{Si-H}}$	1.56 (1.55) [1.52]	1.55 (1.55) [1.52]	1.50	1.50	1.50
$d_{\text{Si-Si}}$				2.15	2.32
α_{HSiH}		90.6° (91.5°) [92.1]	109.5° [109.5°]	114.3°	108.7°
α_{SiSiH}				119.7°	110.2°
$\omega_{\text{wag, bend}}$		954 (980) [999]	829-848 [914, 975]	852, 895	799, 901
ω_{stretch}	1942 (1931) [2042]	1977, 1986 (1958, 1960) [1993, 1996]	2190, 2200 [2187, 2191]	2191, 2219	2174, 2191

experimental structural parameters and vibration frequencies for SiH, SiH_2, and SiH_4.[36] The overall agreement between the DZVP results and experiment is satisfactory, although the calculated bonds are generally longer and the vibration frequencies too low. The largest discrepancy is in the simplest molecule SiH.The use of gradient-corrected modification to the LSD approximation leads to negligible changes in the structure and changes in the vibration frequencies of up to 1%, and we give results for SiH and Si_2H_2 for the BLYP approximation[35] as examples in Table II.

2. Energy eigenvalues

The spectrum of the energy eigenvalues can be obtained readily from electronic structure calculations, although the relationship to measurable quantities is less immediate. The effects of increasing cluster size on the HOMO-LUMO gap (the energy difference between the eigenvalues of the highest occupied and lowest unoccupied orbitals) and the valence bandwidth are shown in Fig. 5, which shows the variation as the number of Si atoms n_{Si} increases. The largest structure we have studied [$Si_{84}H_{64}$, 3(a)] has a HOMO-LUMO gap of 2.88 eV. This and the other values for this cluster differ significantly from those of bulk Si (valence band width 11.98 eV, direct band gap 2.51 eV, indirect band gap 0.61 eV).[37] Pseudopotential calculations with partial structural relaxation show that the convergence to the bulk band gap is indeed very slow,[23] with the gap for $n=525$ being ~ 1.5 eV. The underestimate of the band gap is a familiar shortcoming of the LD approximation, but the bandwidth is in reasonable agreement with optical data.[37]

The general features of the densities of states are similar for the six clusters shown in Fig. 5, and they—and the band widths and band gaps—are remarkably insensitive to the choice of basis set (DZVP or TZVP). In Fig. 6 we compare the density of occupied states for several clusters, and we see that there are relatively minor differences between the curves for decamantane (solid curve) and superpolymantane (dotted curve). Energy eigenvalue densities of states are often compared with x-ray photoemission spectroscopy (XPS) spectra, although the former do not incorporate transition matrix elements, and quantitative agreement cannot be expected. Nevertheless, the present calculations agree much better with XPS measurements for amorphous hydrogenated Si than do the results of semiempirical AM1 calculations,[30] which have much larger gaps and narrower valence bandwidths.

3. Vibration frequencies

The vibration modes that are infrared active reflect the frequencies and types found in small Si/H molecules (see Table II) and occur in three main regions: (a) 600–750 cm^{-1}, Si-H bending and Si-H_2 wagging modes, (b) 800–900 cm^{-1}, Si-H_2 scissor bending modes, and (c) 2000–2175 cm^{-1}, Si-H stretch modes. Mixing of the different mode types is very common. There are, of course, many modes at lower frequency that correspond to Si-Si vibrations,

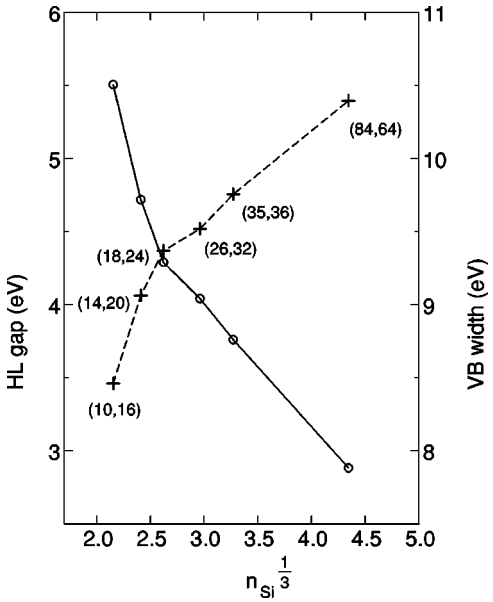

FIG. 5. HOMO-LUMO gap (circles, full curve, left scale) and valence band width (crosses, dashed curve, right scale) as a function of cluster size. The quantity n_{Si} is the number of Si atoms in the cluster.

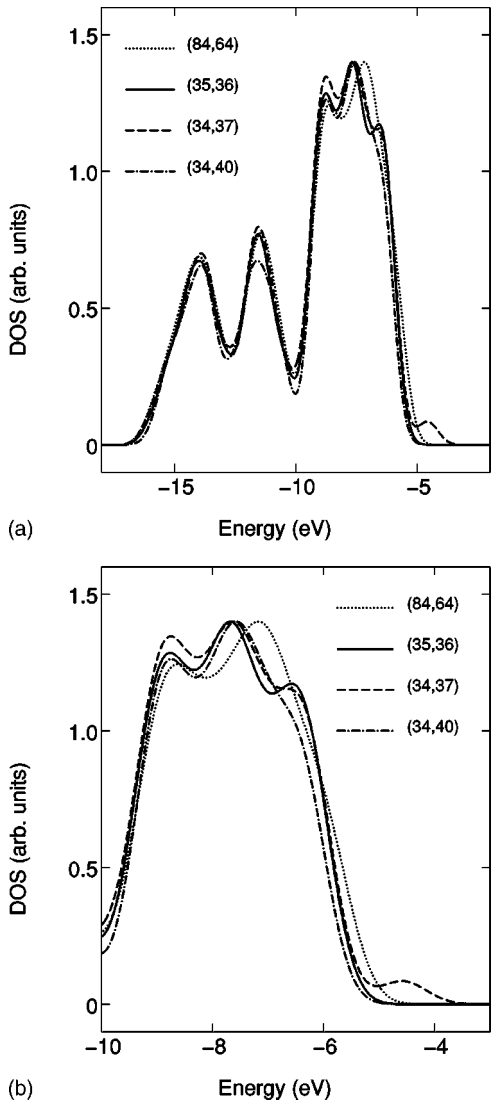

FIG. 6. Energy DOS for clusters (84,64) [dotted] and (35,36) [solid], together with two obtained from the latter by adding one (dashed, majority spin only) and four (dash-dotted) H atoms. (a) Energy range -18 eV to -2 eV; (b) -10 eV to -3 eV.

but their IR activity is generally negligible. The use of DZVP and TZVP basis sets results in very similar vibration frequencies, the latter leading to frequencies that are slightly (less than 1%) below the DZVP values. The vibration spectra for the DZVP basis are shown for these clusters in Figs. 7(a)–7(c), corresponding to the above three regions. Each frequency is represented by a Gaussian peak with full width at half maximum (FWHM) of 10 cm^{-1}, multiplied by the calculated infrared intensity. For comparison purposes we show the vibration frequencies of several small Si/H molecules in Table II.

We have noted above that structural changes with increasing cluster size are not uniform (see Table I). For example, in pentamantane (26,32) there are more Si atoms bonded to *two* H than to a single H atom, while decamantane (35,36), the next in the sequence, has only one quarter as many. The variation in the number of Si-H and Si-H_2 groups in this size range will, of course, be reflected in the physical properties such as the vibration frequencies shown in Fig. 7.

Some trends with increasing cluster size are apparent. There is a pronounced peak above 2150 cm^{-1} in the clusters to pentamantane, with a second peak that moves down in energy from 2147 cm^{-1} in (10,16) to 2122 cm^{-1} in (26,32). The IR spectrum of decamantane (35,36) in this range is markedly different, reflecting the different ratio of Si/H atoms.

B. Clusters with vacancies and additional H atoms

We discuss here the effects of removing one Si atom from the decamantane cluster, adding one to four H atoms to the resulting vacancy, and removing two Si atoms from superpolymantane. We also study the structures and energies of clusters obtained by moving one of the external H atoms in each cluster to a free site inside the vacancy. All of these structures were calculated with both the DGauss and CPMD programs using the LD approximation (LSD in the case of open shells).

1. Structures

Studies of the single vacancy in crystalline Si have often been carried out using the supercell approach, where the vacancy is located at the center of a periodically repeated unit cell. We have noted above that the structure and formation energy converge very slowly as the size of the unit cell and the number of *k* points in the Brillouin zone increase. Puska *et al.*[5] have shown recently that changing these quantities led to the distances between the ions neighboring the vacancy between 2.47 Å and 4.27 Å (the symmetry could be T_d, D_{2d}, C_{3v}, C_{2v}, or lower), the relative volume changes from $+11.7\%$ to -44%, and the heat of formation from 0.93 eV to 3.98 eV. The most reliable results led to a structure with approximately D_{2d} symmetry and Si-Si distances ranging from 2.90 Å to 3.38 Å.

The D_{2d} symmetry of the decamantane molecule [Fig. 2(a)] is unchanged when the central atom is removed [2(b)]. The relaxation in this molecule is greater than in the converged supercell calculations: The pair of atoms that move towards each other are 2.43 Å apart, and each is 3.52 Å from the atoms in the other pair. External H atoms are not shown in Fig. 4 in order to show clearly the significance of adding internal H atoms, which is to cause a relaxation outwards from the vacancy. The symmetries of the VH, VH_2, VH_3, and VH_4 structures are C_s, C_{2v}, C_{3v}, and $\sim T_d$, respectively, in reasonable agreement with those determined by EPR measurements in bulk systems.[17]

The largest cluster we have studied is $Si_{84}H_{64}$ [Fig. 3(a)], and we have also performed calculations for structures obtained by removing two Si atoms (82,64). The ideal neutral divacancy V_2^0, obtained by removing adjacent atoms in bulk Si, has D_{3d} symmetry and two doubly degenerate levels (e_u,e_g). The e_u and e_g levels contain two and zero electrons, respectively, and a Jahn-Teller distortion to C_{2h} symmetry is favored. The nature of the distortion depends on the ordering of the C_{2h} levels (a_u, b_u from e_u; a_g, b_g from e_g), and—as in the case of the single vacancy—the calculated structures and energies of the divacancy depend sensitively on the size

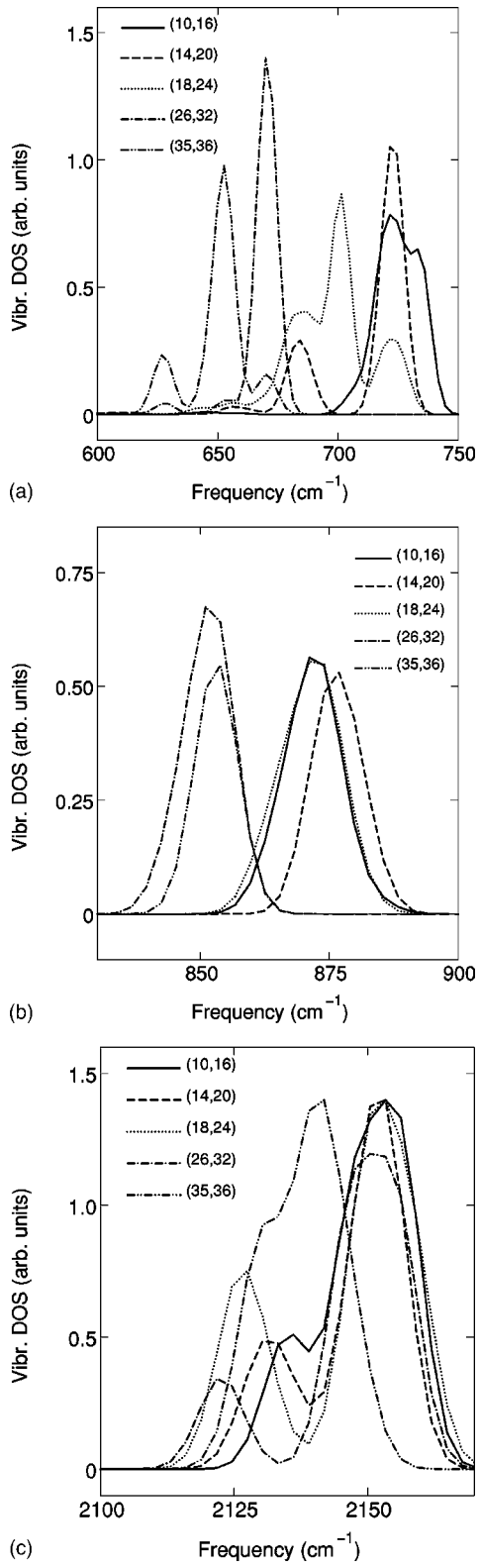

FIG. 7. Calculated infrared vibration spectra for Si_mH_n (m,n) for frequency ranges (a) 600–750 cm^{-1}, (b) 830–900 cm^{-1}, and (c) 2100–2175 cm^{-1}. Full curve (10,16), dashed (14,20), dotted (18,24), dash-dotted (26,32), and dash-double dotted (35,36). The frequencies are represented by a Gaussian peak with FWHM 10 cm^{-1} multiplied by the calculated IR intensity. The curves are scaled to have their maximum values at 1.4 units.

of the cluster or supercell and the orbital basis used.[9,38]

The removal of two adjacent atoms from $Si_{84}H_{64}$ results in a cluster that has lower symmetry than the bulk. This structure has been optimized by the pseudopotential CPMD program, followed by refinement using the all-electron DGauss program. This is the only instance in the present study where the structures obtained by the two approaches were not in excellent agreement. This reflects the subtle nature of the Jahn-Teller distortions found by other authors, as well as the larger relaxations allowed by the open boundary conditions of a cluster. The lowest energies found were for the structures 3(b) (CPMD) and 3(c) (all-electron). The energy difference between all-electron calculations for the two structures was only ~ 0.2 eV.[39]

Structure 3(c) shows similarities to the large pairing Jahn-Teller distortions found in earlier work.[9] The six nearest neighbors of the divacancy have approximately C_{2h} symmetry, although the relaxations in the cluster are again larger than in the bulk. In the all-electron calculations this structure converted to 3(b), and the immediate neighbors of the divacancy again have a symmetry close to C_{2h}. However, the pair of fivefold coordinated Si atoms have approximately D_{4d} symmetry, with the HOMO having near *ungerade* symmetry about the center of the defect, while the LUMO has *gerade* symmetry.

The remaining cluster [(82,64), Fig. 3(d)] was generated from superpolymantane by removing two atoms that were separated by 4.50 Å. The fully relaxed structure has a HOMO-LUMO gap of 1.44 eV and shows similar distortions to those found in the single vacancy. The shortest distances between the ions neighboring the vacancies are ~ 2.57 Å, so that the relaxation from the bulk Si structure is less than in the single vacancy calculation discussed above.

2. Energies and energy eigenvalues

The calculated total energies of the clusters can be used to estimate the formation energies of some defects. In the case of the single vacancy, the energy difference between 2(a) and 2(b), when corrected for the LD value of the cohesive energy of Si,[40] is just over 2.0 eV, compared with the experimental value of 3.6 ± 0.2 eV.[41] In the case of the vacancy pair in 3(b), the formation energy estimated in the same way is 3.0 eV per vacancy. Structure 3(d) is less stable than 3(c) by ~ 1.2 eV. Vacancy clustering is well known in Si, and recent calculations on systems with up to 35 vacancies gave a binding energy of the divacancy of 1.6 eV.[42]

We have also studied the energy differences between the structures 2(b) and 4(a)–4(c) and those obtained by transferring an external H atom to an internal site, e.g. the energy of 4(c) with the structure with one less surface atom and four H atoms surrounding the vacancy. In all cases it is energetically more favorable for the ''mobile'' atom to be on the surface. In structures 4(a) and 4(c) the differences are ~ 0.1 eV. In 2(b) and 4(b) we studied several alternative structures. In these cases the structures with the ''mobile'' atom on the surface were significantly (up to 1 eV) more stable.

We have seen in Sec. III A 2 that there are large HOMO-LUMO gaps in clusters based on the bulk Si structure. They decrease with increasing cluster size, the result for decaman-

tane (35,36) being 3.76 eV. Defect structures often lead to states in the gap of bulk Si,[21] and it is not surprising that the situation in the defect clusters is less uniform. Structures 2(b) and 4(b) and 4(d) have gaps of more than 3 eV. On the other hand, the open-shell structures 4(a) and 4(c) have different occupancies of up- and down-spin electrons, and the overall band gaps of less than 1 eV. The highest occupied orbital in these two structures is also different in these two cases, where it is localized to the region of the ''vacancy'' not occupied by H atoms [in 4(c) the HOMO is symmetric about the axis joining the internal H atom to its Si neighbor]. In cases other than 4(a) and 4(c) the HOMO extends over the whole cluster.

The energy eigenvalues are often useful in interpreting experimental measurements, such as photoemission data, in particular where changes in the system occur.[43] In Fig. 6(b) we show that the DOS for decamantane and the vacancy structure derived from it with additional one (dashed) and four (dash-dotted) H atoms are similar. The differences for the open-shell structure with one H atom are pronounced, as we noted above.

3. Vibration frequencies

The vibration frequencies can provide invaluable information about the structure of any material. For defect structures in Si the frequencies determined by Fourier transform infrared spectroscopy[17,16] (FTIR) have been assigned to VH 2038.5 cm^{-1}; VH_2 2121, 2145 cm^{-1}; VH_3 2155, 2182 cm^{-1}; VH_4 2223 cm^{-1}. Scaled values of semiempirical (MNDO/3) calculations[44] agree reasonably well with measured values. DF calculations with the Harris functional calculations[45] overestimate the measured values by approximately 100 cm^{-1}: VH 2168 cm^{-1}; VH_2 2268 cm^{-1}; VH_3 2301 cm^{-1}; VH_4 2334 cm^{-1}.

Suezawa has performed optical absorption measurements on Si after irradiation by high-energy electrons. While the peak at 2122 cm^{-1} is also assigned by him to VH_2,[46] he attributes lines at 2223 cm^{-1} and 2166 cm^{-1} to self-interstitials with four (IH_4) and three (IH_3) H atoms, respectively.[47] This conclusion was disputed recently by Hourahine *et al.*,[48] who calculated that the stretch modes of interstitial silane (SiH_4) were lowered by 300 cm^{-1} from those of the isolated molecule ($\sim$2000 cm^{-1}, see Table II).

In Fig. 8 we show the calculated IR spectra of defect structures based on decamantane (35,36). The removal of a Si atom results in a structure with lower symmetry, the number of infrared active modes and their spread are increased, and a mode appears at 2103 cm^{-1} that is absent in decamantane. The reduction in the number of neighbors should strengthen the remaining bonds and increase the corresponding vibration frequencies. In fact, the average frequencies of the infrared active modes near 650, 850, and 2140 cm^{-1} are increased by up to 10 cm^{-1}. Changes of this magnitude are accessible to IR measurements, although the correlation with a particular defect structure is not straightforward.[49] As the number of H atoms increases there are distinctive changes in the relative strengths of peaks near 630, 660, 690, and 860 cm^{-1}. Particularly striking is the appearance in VH_4 of

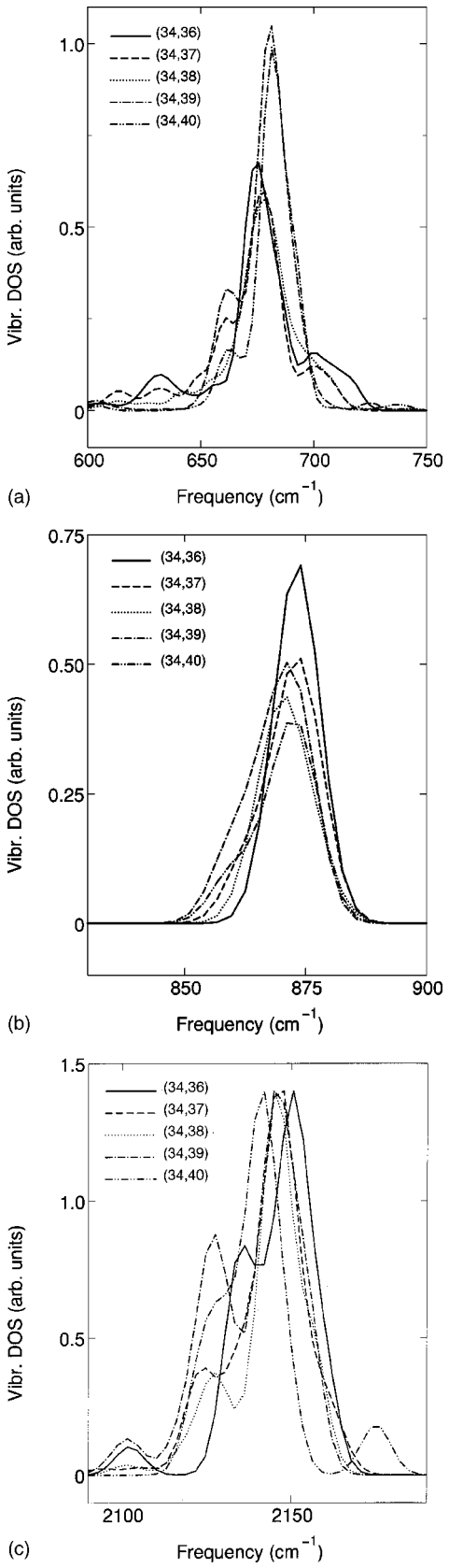

FIG. 8. Calculated infrared vibration spectra of Si_mH_n clusters. (a) 600–750 cm^{-1}; (b) 830–900 cm^{-1}; (c) 2080–2180 cm^{-1}. Full curve (34,36), dashed (34,37), dotted (34,38), dash-dotted (34,39), and dash-double dotted (34,40). See caption of Fig. 7.

a peak of higher energy (2175 cm^{-1}) that is absent in the other defect structures.

The difficulty in comparing vibration frequencies with experiment is reflected in the scaling approach often used, and we have noted above the dependence of the calculated vibration frequencies on the choice of basis (DZVP and TZVP differ by $\sim 1\%$) and functional (all the cluster results given were obtained with the LSD approximation). In the present case the frequencies appear to be ~ 50 cm^{-1} lower than the measured values in the range ~ 2100 cm^{-1}, but we expect that the trends they show should be reliable.

IV. DISCUSSION AND CONCLUDING REMARKS

We have described an extensive series of all-electron density functional calculations on the structures and energies of Si/H clusters with up to 148 atoms. The positions of all atoms are allowed to relax during structural optimization, and vibration frequencies and infrared intensities have been determined for clusters with up to 74 atoms. The calculations were motivated by our interests in the properties of defects in bulk Si and in amorphous hydrogenated Si. While clusters of this size cannot describe all such properties realistically, energy changes as well as the changes in the lineshapes and relative locations of the IR absorption bands provide much useful information.

The calculations support earlier assessments that clusters of 150 atoms are too small to calculate some properties of bulk Si, since the open boundary conditions of the clusters allow greater structural relaxations than in the bulk. The tetrahedral clusters, however, provide a very good description of Si-Si and Si-H bond lengths, as well as the bond angles. In the case of the neutral vacancy, up to four H atoms can saturate the available dangling bonds. In all cases, these H atoms have a lower energy when they move to a vacant site on the surface of the cluster. We note that the Staebler-Wronski effect has been attributed to radiation damage to the surface followed by migration of H that leaves behind vacancies with dangling bonds that could act as traps for carriers. This picture is consistent with the present results, although additional calculations would have to be performed to determine the energy barriers and optimum paths for diffusion from the vacancy to the surface.

Vibration frequencies can provide detailed structural information, and we believe that the present calculations are the first for these systems using a method without adjustable parameters. The calculated frequencies show distinctive trends with changing structures that should be useful as ''fingerprints'' in analyzing IR data. Most of the H atoms in these model systems are on the ''surface'' of the clusters, and some vibration frequencies should be observable in the IR spectra of Si surfaces with chemisorbed hydrogen. Examples of such measurements are given in Ref. 50.

Calculations of the vibration frequencies for larger systems are very difficult with the present generation of computers, so that the use of semiempirical methods (e.g. force field fitted to experimental data, or parametrized molecular orbital methods such as AM1) will remain useful alternatives for studies of, in particular, the degradation mechanisms that occur in *a*-Si:H.

ACKNOWLEDGMENTS

The calculations were performed on Cray T90 and T3E computers in the Forschungszentrum Jülich with generous grants of CPU time from the Forschungszentrum and the John von Neumann-Institut für Computing (NIC). R.O.J. thanks W. Beyer and H. Wagner (ISI-PV, FZ Jülich) for helpful discussions, and J. Docter (NIC) for essential assistance with the calculations with the largest demands on memory and CPU time.

[1] S.K. Estreicher, Phys. Status Solidi B **217**, 513 (2000).
[2] See, for example, G. D. Watkins, in *Deep Centers in Semiconductors*, edited by S. T. Pantelides (Gordon and Breach, New York, 1986), p. 147.
[3] S. Öğüt, H. Kim, and J.R. Chelikowsky, Phys. Rev. B **56**, R11353 (1997).
[4] J.L. Mercer, J.S. Nelson, A.F. Wright, and E.B. Stechel, Modell. Simul. Mater. Sci. Eng. **6**, 1 (1998).
[5] M.J. Puska, S. Pöykkö, M. Pesola, and R.M. Nieminen, Phys. Rev. B **58**, 1318 (1998).
[6] A. Antonelli, E. Kaxiras, and D. J. Chadi, Phys. Rev. Lett. **81**, 2088 (1998).
[7] A. Zywietz, J. Fürthmüller, and F. Bechstedt, Phys. Status Solidi B **210**, 13 (1998).
[8] H. Seong and L.J. Lewis, Phys. Rev. B **53**, 9791 (1996) (simple and split divacancies).
[9] S. Öğüt and J.R. Chelikowsky, Phys. Rev. Lett. **83**, 3852 (1999).
[10] D.L. Staebler and C.R. Wronski, Appl. Phys. Lett. **31**, 292 (1977).
[11] See, for example, R. Biswas and Y.-P. Li, Phys. Rev. Lett. **82**, 2512 (1999), and references therein.
[12] B.W. Clare *et al.*, Thin Solid Films **288**, 76 (1996).
[13] H.M. Branz, Solid State Commun. **105**, 387 (1998).
[14] B. Tuttle and C.G. Van de Walle, Phys. Rev. B **59**, 12884 (1999).
[15] A.N. Safonov and E.C. Lightowlers, Mater. Sci. Eng., B **36**, 251 (1996). These measurements identified luminescence centers containing two, three, and four H atoms in radiation-damaged Si.
[16] P. Stallinga, P. Johannesen, S. Herstrøm, K. Bonde Nielsen, B. Bech Nielsen, and J.R. Byberg, Phys. Rev. B **58**, 3842 (1998).
[17] B. Bech Nielsen, L. Hoffmann, and M. Budde, Mater. Sci. Eng., B **36**, 259 (1996); See also, M. Budde, B. Bech Neilsen, J.C. Keay, and L.C. Feldman, Physica B **273-274**, 208 (1999).
[18] B. Bech Nielsen, P. Johannesen, P. Stallinga, K. Bonde Nielsen, and J.R. Byberg, Phys. Rev. Lett. **79**, 1507 (1997).
[19] W. Beyer, Semicond. Semimetals **61**, 165 (1999).
[20] M. Peressi, M. Fornari, S. de Gironcoli, L. de Santis, and A. Baldereschi, Philos. Mag. B **80**, 515 (2000), and references therein.
[21] P.L. Silvestrelli, N. Marzari, D. Vanderbilt, and M. Parrinello, Solid State Commun. **107**, 7 (1998).

[22] R.P. Messmer and G.D. Watkins, Phys. Rev. B **7**, 2568 (1973).
[23] S. Öğüt, J.R. Chelikowsky, and S.G. Louie, Phys. Rev. Lett. **79**, 1770 (1997).
[24] R. Martoňák, C. Molteni, and M. Parrinello, Phys. Rev. Lett. **84**, 682 (2000).
[25] B.W. Clare, G. Talukder, P.J. Jennings, J.C.L. Cornish, and G.T. Hefter, J. Comput. Chem. **15**, 644 (1994).
[26] B.W. Clare, P.J. Jennings, J.C.L. Cornish, G.T. Hefter, and D.J. Santjojo, J. Comput. Chem. **17**, 306 (1996).
[27] A recent example is the study of carbon clusters with up to 32 atoms; R. O. Jones, J. Chem. Phys. **110**, 5189 (1999).
[28] J.J.P. Stewart, QCPE Bull. **10**, 86 (1990).
[29] M.J.S. Dewar, E.G. Zoebisch, E.F. Healy, and J.J.P. Stewart, J. Am. Chem. Soc. **107**, 3902 (1985).
[30] B.W. Clare, P.J. Jennings, J.C.L. Cornish, G. Talukder, C.P. Lund, and G.T. Hefter, J. Comput. Chem. **14**, 1423 (1993).
[31] CPMD program version 3.0, J. Hutter *et al.*, Max-Planck-Institut für Festkörperforschung and IBM Research 1990-2000.
[32] N. Troullier and J.M. Martins, Phys. Rev. B **43**, 1993 (1991).
[33] DGauss program, UniChem package of Oxford Molecular Group (DZVP: double zeta basis with polarization functions, auxiliary basis A1; TZVP: triple zeta basis with polarization functions TZVP, auxiliary basis A2). LSD approximation: S.H. Vosko, L. Wilk, and M. Nusair, Can. J. Phys. **53**, 1385 (1980).
[34] A. Komornicki and G. Fitzgerald, J. Chem. Phys. **98**, 1398 (1993).
[35] A.D. Becke, J. Chem. Phys. **88**, 2547 (1988); C. Lee, R.G. Parr, and W. Yang, Phys. Rev. B **37**, 785 (1988).
[36] Experimental values are from the *NIST Chemistry WebBook, NIST Standard Reference Database Number 69*, edited by W. G. Mallard and P. J. Linstrom (National Institute of Standards and Technology, Gaithersburg, MD, 2000) (http://webbook.nist.gov).
[37] P.R.C. Kent, R.Q. Hood, M.D. Tower, R.J. Needs, and G. Rajagopal, Phys. Rev. B **57**, 15293 (1998).
[38] M. Pesola, J. von Boehm, S. Pöykkö, and R.M. Nieminen, Phys. Rev. B **58**, 1106 (1998).
[39] Structure 3(c) is also found to be the most stable if the CPMD program is used with the gradient-corrected functional of J.P. Perdew, K. Burke, and M. Ernzerhof, Phys. Rev. Lett. **77**, 3865 (1996). This structure was found by long simulated annealing runs starting from both (a) the bulk structure with two adjacent atoms removed, and (b) structure 3(b).
[40] X.-P. Li, D.M. Ceperley, and R.M. Martin, Phys. Rev. B **44**, 10929 (1991) give a value of 5.30 eV.
[41] G.D. Watkins and J.W. Corbett, Phys. Rev. **134**, A1359 (1964); S. Dannefaer, P. Mascher, and D. Kerr, Phys. Rev. Lett. **56**, 2195 (1986).
[42] A. Bongiorno, L. Colombo, and T. Diaz de la Rubia, Europhys. Lett. **43**, 695 (1998).
[43] See, for example, B.W. Clare, P.J. Jennings, C.P. Lund, J.C.L. Cornish, and G.T. Hefter, Thin Solid Films **326**, 160 (1998).
[44] P. Deák, M. Heinrich, L.C. Snyder, and J.W. Corbett, Mater. Sci. Eng., B **4**, 57 (1989). The scaled frequencies are VH 2057 cm^{-1}; VH_2 2080, 2076 cm^{-1}; VH_3 2106, 2095 cm^{-1}; VH_4 2109, 2094 cm^{-1}.
[45] Y.K. Park, S.K. Estreicher, C.W. Myles, and P.A. Fedders, Phys. Rev. B **52**, 1718 (1995). These calculations adopted a spin-averaged, non-self-consistent scheme using the Harris functional and the local density approximation. Nonlocal pseudopotentials and a minimum basis of localized atomiclike functions (one *s* and three *p* functions per site) were used.
[46] M. Suezawa, Jpn. J. Appl. Phys., Part 2 **38**, L758 (1999).
[47] M. Suezawa, Jpn. J. Appl. Phys., Part 2 **37**, L806 (1998).
[48] B. Hourahine, R. Jones, S. Öberg, and P.R. Briddon, Phys. Rev. B **59**, 15729 (1999).
[49] H. Wagner, ISI-PV, Forschungszentrum Jülich (private communication).
[50] S. Watanabe, J. Chem. Phys. **108**, 5965 (1998).